Contribution from the Central Salt and Marine Chemicals Research Institute, Bhavnagar 364 002, India

Equilibrium and Electrochemical Studies on the Complexes Formed by the Interaction of K[Ru(EDTA-H)Cl]·2H_2O with Oxygen and Hydrogen Peroxide

M. M. Taqui Khan,* Amjad Hussain, G. Ramachandraiah, and M. A. Moiz

Received April 25, 1985

The interaction of O_2 and H_2O_2 with the complex K[Ru(EDTA-H)Cl]·2H_2O (**1**) has been studied in aqueous solution by potentiometry, spectrophotometry, and electrochemical and gas absorption techniques at 25 °C and μ = 0.10 M (KCl). Complex **1** undergoes fast aquation in solution to form the complex [Ru(EDTA-H)H_2O] (**2**). Acid dissociation and hydrolysis constants of complex **2** calculated under nitrogen atmosphere are reported. The dissociation of a carboxylate proton from **2** forms the anionic species $[Ru(EDTA)(H_2O)]^-$ (**2a**). Hydrolysis of **2a** results in the formation of the monohydroxo and dihydroxo complexes $[Ru(EDTA)(OH)]^{2-}$ (**2b**) and $[Ru(EDTA)(OH)_2]^{3-}$ (**2c**), respectively. Complex **2b** reversibly combines with oxygen in the pH range 7–9.5 to form a hydroxo–μ-peroxo–Ru(IV) species $[(EDTA)(OH)Ru^{IV}(O_2^{2-})Ru^{IV}(OH)(EDTA)]^{4-}$ (**3**). The formation of **3** is supported by equilibrium, spectrophotometric, and electrochemical data. At pH values greater than 9.5 a dihydroxo–μ-peroxo–Ru(IV) complex $[LRu^{IV}(OH)_2]_2O_2$ (**3a**) is formed and decomposes irreversibly to the monomeric dihydroxo species $[LRu^{III}(OH)_2]^{2-}$ (**2c**) with the release of molecular oxygen. When H_2O_2 is added to complex **2** in the ratio 1:0.5 a μ-hydroperoxo–Ru(III) complex of composition $[(EDTA\text{-}H)Ru^{III}(H_2O_2)Ru^{III}(EDTA\text{-}H)]$ (**4**) is formed in the acidic range. Addition of H_2O_2 to **2** in the ratio of 1:1, however, results in the formation of the μ-peroxo–Ru(IV) complex $[(EDTA\text{-}H)Ru^{IV}(O_2^{2-})Ru^{IV}(EDTA\text{-}H)]$ (**5**). Complexes **4a** and **5a** undergo stepwise hydrolysis in solution and form the dihydroxo complexes **4b** and **5b** and the tetrahydroxo complexes **4c** and **5c**, respectively. Complexes **4c** and **5c** decompose slowly to complex **2c** at pH 9.5. A tetradentate coordination of EDTA and a six-coordination for Ru(III) and Ru(IV) are proposed in the peroxo complexes **4b** and **5b**. Complex **5** has been isolated in the solid state and characterized.

Introduction

In recent years there has been a growing interest in the study of dioxygen complex of transition metals because of the important role played by such complexes in a number of biological and chemical reactions.[1-7] The respiratory process of higher animals depends solely on the formation of reversible dioxygen metal complexes for the supply of oxygen to necessary sites in oxygen metabolism.[8] Formation of a metal dioxygen complex has been reported in the photosystem II of photosynthesis for splitting water.[9,10] The synthetic metal complexes of dioxygen serve as models in a variety of reactions. They have a potential use in photochemical cells for the decomposition of water and the metal–air batteries.[11,12] The complexes also serve as oxidizing agents and as intermediates in oxidation of a variety of organic compounds.[13,14] Consequent with their importance outlined above these complexes have been studied by a number of physicochemical techniques[1-3] like potentiometry, spectrophotometry, polarography, cyclic voltammetry, ESR, and X-ray to investigate the nature of complexes formed in solution and their thermodynamic stability and the nature of bonding of dioxygen to the metal ion.

Dioxygen complexes that have been most thoroughly studied are those of Co(II),[1-3,15-21] Fe(II),[21-23] and Mn(II).[5,24] The studies of the complexes of heavier 4d and 5d transition metal ions were mostly confined to the complexes of Rh(I),[25] Ir(I),[26] Pt(0),[27] Pd(0),[28] and Ru(0).[29]

Ezerskaya and Solovykh[30a] studied the interaction of K-$[Ru^{III}(EDTA\text{-}H)Cl]\cdot 2H_2O$ (**1**) with H_2O_2[30b,c] and molecular oxygen[30d,f] at different pH values and temperatures in solution. In the presence of H_2O_2, at pH 3–5 formation of complexes of the composition $[Ru^{III}(EDTA\text{-}H)]_2O_2$ and $[(EDTA\text{-}H)Ru^{III}(O_2^{\bullet-})Ru^{IV}(EDTA\text{-}H)]$ was suggested. The reaction of **1** with oxygen was found to be reversible in the pH range 7–10 with a decrease in oxygen uptake on increasing the pH and temperature.[30d,e] In the presence of molecular oxygen a complex of the composition [(EDTA)Ru(OH)O_2Ru(EDTA)] was reported.[30a]

(1) Taqui Khan, M. M.; Martell, A. E. *Homogeneous Catalysis by Metal Complexes*; Academic: New York, 1974; Vol 1.
(2) Spiro, T. G., Ed. *Metal Ion Activation of Dioxygen*; Plenum: New York, 1980.
(3) Taqui, Khan, M. M.; Martell, A. E. *Dioxygen Complexes*; Plenum: New York 1986, in press.
(4) McLendon, G.; Martell, A. E. *Coord. Chem. Rev.* **1976**, *19*, 1.
(5) James, R. D.; Summerville, D. A.; Basolo, F. *Chem. Rev.* **1979**, *79*, 139.
(6) Wilshire, J.; Sawyer, D. T. *Acc. Chem. Res.* **1979**, *12*, 105 and references therein.
(7) Taqui Khan, M. M. Plenary Lecture on "Catalysed Oxidation with Ruthenium(III) Dioxygen Complexes" presented at 4th International Symposium on Homogeneous Catalysis, Leningrad, USSR, Sept 1984.
(8) Senozen, N. M. *J. Chem. Educ.* **1974**, *51*, 503; **1976**, *53*, 684, **1979**, *56*, 748.
(9) Ruben, S.; Randall, M.; Kamen, M.; Hyde, J. L. *J. Am. Chem. Soc.* **1941**, *63*, 877.
(10) Health, R. L. *Ini. Rev. Cytol.* **1973**, *34*, 49.
(11) Sawyer, D. T.; Seo, E. T. *Inorg. Chem.* **1977**, *16*, 499.
(12) Taqui Khan, M. M. *J. Indian Chem. Soc.* **1982**, 59, 160.
(13) Taqui Khan, M. M.; Bajaj, H. C. *React. Kinet. Catal. Lett.* **1985**, *28*, 339. Taqui Khan, M. M.; Prakash Rao, A. *J. Mol. Catal.* **1986**, *35*, 237. Taqui Khan, M. M.; Shukla, R. S. *J. Mol. Catal.*, in press. Taqui Khan, M. M.; Shukla, R. S. *J. Mol. Catal.* **1986**, *34*, 19. Taqui Khan, M. M.; Siddiqui, M. R. H.; Amjad Hussain.; Moiz, M. A. *Inorg. Chem.*, in press.
(14) Martell, A. E. *Pure Appl. Chem.* **1983**, *55*, 125.
(15) Martell, A. E. *Acc. Chem. Res.* **1982**, *15*, 155. *Chem. Rev.* **1984**, *84*, 137.
(16) Collman, J. P.; Gagne, R. R.; Kouba, J.; Wahren, H. L. *J. Am. Chem. Soc.* **1974**, *96*, 6800.
(17) Miskowski, V. M.; Robbins, J. L.; Treitel, I. M.; Gray, H. B. *Inorg. Chem.* **1975**, *14*, 2318. Abrahamson, H. B.; Frazler, C. C.; Ginley, D. S.; Gray, H. B.; Lilienthal, J.; Tyler, D. R.; Wrighton, M. S. *Inorg. Chem.* **1977**, *16*, 1554. Lever, A. B. P.; Ozin, G. A.; Gray, H. B. *Inorg. Chem.* **1980**, *19*, 1823.
(18) McLendon, G.; Pickens, S. R.; Martell, A. E. *Inorg. Chem.* **1977**, *16*, 1551. McLendon, G.; MacMillan, D. T.; Hariharan, M.; Martell, A. E. *Inorg. Chem.* **1975**, *14*, 2322.
(19) Roberts, D. A.; Bush, J. M.; Tsao, Y.-Y. Katovic, V.; Fortman, J. J. *Inorg. Chem.* **1983**, *22*, 1804.
(20) Chen, L. S.; Koehler, M. E.; Pestel, B. C.; Cummings, S. C. *J. Am. Chem. Soc.* **1978**, *100*, 7243.
(21) Basolo, F.; Hoffman, B. M.; Ibers, J. A. *Acc. Chem. Res.* **1975**, *8*, 384.
(22) Collman, J. P.; Gagne, R. R.; Reed, C. A.; Halbert, T. R.; Lang, G.; Robinson, W. T. *J. Am. Chem. Soc.* **1975**, *97*, 1427.
(23) Collman, J. P. *Acc. Chem. Res.* **1968**, *1*, 136. Tsuchida, E.; Honda, K. *Chem. Lett.* **1975**, 119. Welborn, C. H.; Dolphin, D.; James, B. R. *J. Am. Chem. Soc.* **1981**, *103*, 2869.
(24) McAuliffe, C. A. *J. Organomet. Chem.* **1982**, *228*, 255.
(25) Nakamura, A.; Tatsumo, Y.; Otsuko, S. *Inorg. Chem.* **1972**, *11*, 2058. Bennett, M. J.; Donaldson, P. B. *Inorg. Chem.* **1977**, *16*, 1581.
(26) Mague, J. T.; Wilkinson, G. *J. Chem. Soc. A* **1966**, 1736. McGinnety, J. A.; Payne, N. C.; Ibers, J. A. *J. Am. Chem. Soc.* **1969**, *91*, 6308; Taqui Khan, M. M.; Martell, A. E. *Inorg. Chem.* **1974**, *13*, 2961; *Inorg. Chem.* **1975**, *14*, 676. Taqui Khan, M. M.; Rafiq, Mohiuddin.; Mehreen, Ahmed.; Martell, A. E. *J. Coord. Chem.* **1980**, *10*, 1.
(27) Claris, H. C.; Goel, A. B.; Wong, C. S. *Inorg. Chem. Acta* **1979**, *34*, 159.
(28) Otsuka, S.; Nakamura, A.; Tatsuno, Y. *J. Am. Chem. Soc.* **1969**, *81*, 6994.
(29) Laing, K. R.; Roper, W. R. *Chem. Commun.* **1968**, 1556; **1970**, 1272. Cavit, B. E.; Grundy, K. R.; Roper, W. R. *J. Chem. Soc. Chem. Commun.* **1972**, 60.
(30) (a) Ezerskaya, N. A.; Solovykh, T. P. *Zh. Neorg. Khim.* **1966**, *11*, 1855. (b) *Ibid.* **1966**, *11*, 2197. (c) *Ibid.* **1967**, *12*, 2922. (d) *Ibid.* **1966**, *11*, 1462. (e) *Ibid.* **1968**, *13*, 186. (f) *Ibid.* **1966**, *11*, 2569.

0020-1669/86/1325-3023$01.50/0 Published 1986 by the American Chemical Society

However, supporting physicochemical evidence for the formation of the various complexes cited above in regards to the composition of the species, the oxidation state of the metal ion in the dioxygen complex, and the mode of bonding of dioxygen was not reported.[30a]

We have recently described a new series of dioxygen complexes of ruthenium with a number of amino poly(carboxylic acids).[31] Since K[Ru(EDTA-H)Cl]·2H_2O (**1**) and the corresponding aquo complex [Ru(EDTA-H)(H_2O)] (**2**) are important source materials[32] for the synthesis of a number of Ru(II) and Ru(III) complexes, it was considered important to investigate the solution chemistry of these complexes and their detailed interaction with molecular oxygen and H_2O_2 with a view to elucidate the nature of the species formed in solution. In the present paper the solution chemistry of complex **1** was studied in the pH range 3–11 in the presence of nitrogen and oxygen. The nature of the species formed was elucidated by potentiometry, spectrophotometry, polarography, cyclic voltammetry, and oxygen absorption studies.

The peroxo species formed by the reaction of **1** with H_2O_2 in the mole ratios 1:0.5 and 1:1 in the pH range 3–11 were also investigated by the above techniques. This provided a comparison of the peroxo species of ruthenium formed with dioxygen and H_2O_2 and a unified pattern of the dioxygen complexes formed in different pH ranges.

Experimental Section

Material. Hydrated ruthenium chloride, $RuCl_3 \cdot xH_2O$ was obtained from Johnson-Mathey; Na_2EDTA (AR) and H_2O_2 (30%) were obtained from BDH chemicals. All other reagents used were AR grade. High-purity nitrogen was obtained by passing the gas through alkaline pyrogallate and vanadous sulfate solutions. Oxygen was used as received.

Synthesis. $K_2[RuCl_5H_2O]$ used as the starting material for the synthesis of **1** was prepared by the method of Mercer and Buckley.[33] K[Ru(EDTA-H)Cl]·2H_2O (complex **1**) was prepared by the method of Ezerskaya and Solovykh[30a] as modified by Diamantis et al.[32] The product was characterized by elemental analysis.

Physical Measurement. All pH measurements were made with a Digisun Model DI-707 pH meter correct to 0.01 pH and equipped with a combination glass electrode. The electrode system was calibrated below pH 3.50 and above pH 10.50 by using HCl and NaOH solutions, respectively. Appropriate amounts of complex **1** were dissolved in 50 mL of 0.10 M KCl (μ = 0.10) to prepare a 1 mM solution. The solution was titrated against a carbonate-free NaOH standard while continuously bubbling purified nitrogen or oxygen through the solution. Titrations were also carried out in the ratio of 0.5 equiv (1:0.5) and 1 equiv (1:1) of H_2O_2 to the metal ion. All the titrations were performed in a jacketed cell through which water at a constant temperature of 35 ± 0.1 °C was circulated.

Electrochemical measurements were made with a Princeton Applied Research (PAR) electrochemical instrument equipped with a precision X-Y recorder. A PAR 174A polarographic analyzer was used to record dc and differential-pulse polarograms; a PAR 175 universal programmer coupled with the PAR 174A analyzer was used for recording cyclic voltammograms. A PAR 303 SMDE assembly provided with a DME/HMDE working electrode and platinum wire (0.5 mm diameter) was used. All potentials were measured against a Ag/AgCl reference electrode at 25 °C. A medium-sized drop (2.75 mg mass) was used with an open circuit and a 2-s drop time.

For controlled-potential coulometry (CPL) a PAR Model 173 potentiostat was used to control the potential. Integration of the current–time curve was achieved by means of a PAR Model 179 integrator. A coulometric cell of three-electrode configuration consisting of a mercury-pool working electrode, a Pt-wire counter electrode separated from the main solution by a glass frit, and a SCE reference electrode was used.

The electronic absorption spectra were recorded on a Beckman Model DU-7 high speed UV/vis spectrophotometer. Matched 10-mm quartz cuvettes were used, and the spectra were recorded at 25 °C and μ = 0.10 M (KCl) against a reference of 0.10 M KCl solution.

Oxygen absorption studies were done on a manometric setup consisting of a jacketed glass cell with an inlet and outlet for gas and with an arrangement to monitor pH changes and to add base from an automatic buret. The cell was filled with oxygen, whose uptake was measured at points corresponding to 0.50, 1.00, 1.50, 2.00, and 2.50 mol of base/mol of metal ion on the titration curves in the presence of O_2. The volume changes at constant pressure (atmospheric) corresponding to O_2 absorption were recorded at t = 35 °C and μ = 0.10 M (KCl).

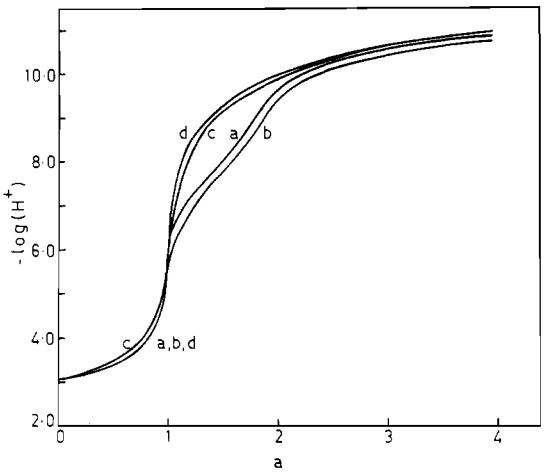

Figure 1. Potentiometric titration curves of K[Ru(EDTA-H)H_2O]·2H_2O (1×10^{-3} M) solution at 35 °C and μ = 0.1 M KCl in the presence of (a) nitrogen, (b) oxygen, (c) 0.5 equiv of hydrogen peroxide, and (d) 1 equiv of hydrogen peroxide.

Results and Discussion

Potentiometry of Complex 1 under N_2. The titration curve of complex **1** under nitrogen (Figure 1a) shows inflections at a = 1.0 and 2.0. The three buffer regions a = 0–1, a = 1–2, and a = 2–3 correspond to equilibria 1–3, respectively, where MHL

$$\underset{\mathbf{2}}{M^{III}HL} \overset{K_1}{\rightleftharpoons} \underset{\mathbf{2a}}{M^{III}L} + H^+ \qquad K_1 = [ML][H^+]/[MHL] \quad (1)$$

$$M^{III}L \overset{K_2}{\rightleftharpoons} \underset{\mathbf{2b}}{LM^{III}OH} + H^+ \qquad K_2 = [LM^{III}OH][H^+]/[ML] \quad (2)$$

$$LM^{III}OH \overset{K_3}{\rightleftharpoons} \underset{\mathbf{2c}}{LM^{III}(OH)_2} + H^+ \qquad K_3 = [LM^{III}(OH)_2][H^+]/[LM^{III}OH] \quad (3)$$

denotes the complex Ru(EDTA-H)(H_2O) (**2**). The charges on the complexes are omitted for the sake of clarity.

The constants log K_1, log K_2, and log K_3 calculated at 35 °C (μ = 0.1 M KCl) by an algebraic method described earlier[34] are −2.36 ± 0.01, −7.86 ± 0.02, and −11.07 ± 0.02, respectively.

EDTA-H acts as a pentadentate ligand[30a,35,36] in complex **1** with Cl^- occupying the sixth coordination position. A high molar conductivity of complex **1** in solution and the ease of replacement of Cl^- by other groups[32] can be explained as being due to lability[32] of the equatorially coordinated Cl^- in solution. On dissolution of complex **1** in water, Cl^- is immediately replaced by a water molecule to form complex **2**. The proton on the uncoordinated carboxylic acid group in **2** is neutralized between a = 0 and a = 1 (Figure 1a) to give complex **2a**. The first and second hydrolysis of complex **2a** take place in separate steps. The first hydrolysis is due to deprotonation of water molecule already coordinated to Ru(III) to give complex **2b**, and the second hydrolysis results from the deprotonation of water molecule coordinated after the carboxylate group is replaced to give complex **2c**. The dissociation constants reported are in good agreement with those reported[37] earlier.

(31) (a) Taqui Khan, M. M.; Ramachandraiah, G. *Inorg. Chem.* **1982**, *21*, 2109. (b) Taqui Khan, M. M. *Pure Appl. Chem.* **1983**, *55*, 159.
(32) Diamantis, A. A.; Dubrawski, J. V. *Inorg. Chem.* **1981**, *20*, 1142.
(33) Mercer, E. E.; Buckley, R. R. *Inorg. Chem.* **1965**, *4*, 1692.
(34) Taqui Khan, M. M.; Amjad Hussain *Indian J. Chem., Sect. A* **1980**, *19A*, 50.
(35) Bailar, J. C.; Sievers, R. E. *Inorg. Chem.* **1962**, *1*, 174.
(36) Ezerskaya, N. A.; Solovykh, T. P.; Evastafence, O. N.; Shubochkin, L. K.; Bebkic, N. K. *Zh. Neorg. Khim.* **1975**, *20*, 1036.
(37) (a) Endicott, J. F.; Taube, H. *Inorg. Chem.* **1965**, *4*, 437. (b) Taqui Khan, M. M; Ramachandraiah, G. *Indian J. Chem., Sect. A* **1982**, *21A*, 41. (c) Shimizu, K.; Matsuban, T.; Sato, G. P. *Bull. Chem. Soc. Jpn.* **1974**, *47*, 1651.

Potentiometry of 1 under O_2. The titration of complex **1** under oxygen gives a curve (Figure 1b) similar to that under nitrogen (Figure 1a) showing inflections at $a = 1$ and $a = 2$. The buffer region $a = 0$–1 exactly overlaps with that under nitrogen, indicating the existence of the same type of equilibrium under nitrogen and oxygen, viz. reaction 1. The value of log K_1 (reaction 1) calculated under O_2 is the same as under N_2, (−2.36). The buffer regions between $a = 1$–2 and $a = 2$–3 under oxygen (Figure 1b), however, lie much below that of the corresponding buffer regions under nitrogen, indicating interaction between the complex and dioxygen. The fact that the titration curve from $a = 1$–3 is independent of the concentration of the complex indicates the formation of a hydroxo–peroxo species **3** in the buffer region $a = 1$–2 and a dihydroxo–μ-peroxo species **3a** in the buffer region $a = 2$–3 as per reactions 4 and 5, respectively (L = EDTA; the

$$2M^{III}L + O_2 \overset{K_4}{\rightleftharpoons} \underset{\mathbf{3}}{(ML^{IV}OH)_2O_2^{2-}} + 2H^+ \quad (4)$$

$$K_4 = [(LM^{IV}OH)_2O_2^{2-}][H^+]^2/[M^{III}L]^2$$

$$(LM^{IV}OH)_2O_2^{2-} + 2H_2O \overset{K_5}{\rightleftharpoons} \underset{\mathbf{3a}}{(LM^{IV}(OH)_2)_2O_2^{2-}} + 2H^+ \quad (5)$$

$$K_5 = [(LM^{IV}(OH)_2)_2O_2^{2-}][H^+]^2/[(LM^{IV}OH)_2O_2^{2-}]$$

charges on the complexes are omitted for the sake of clarity). The constants log K_4 and log K_5 calculated at 35 °C (μ = 0.10 M KCl) by an algebraic method are −11.97 ± 0.02 and −20.56 ± 0.02, respectively.

Complex **2a** undergoes hydrolysis in separate steps between $a = 1$–2 and $a = 2$–3 under oxygen accompanied by a significant decrease in pH as compared to a titration curve under nitrogen (Figure 1a). The depression in pH can be attributed to an increase in the stability of the complex due to a change in the oxidation state of ruthenium from +3 to +4 on interaction with oxygen. The interaction with dioxygen to form a μ-peroxo–Ru(IV) species **3** is supported by oxygen uptake measurements, which show the stoichiometry of metal to oxygen in complex **3** to be 2:1. Solution of **3** on acidification with 3 M HCl liberates H_2O_2 in the ratio of 1 mol of H_2O_2/2 mol of metal ion. The above results indicate that the coordinated oxygen molecule oxidizes two Ru(III) ions in **2b** to a formal Ru(IV) state coordinated to a μ-peroxo species. Complex **2a** undergoes simultaneous oxygenation and hydrolysis to form the μ-peroxo complex **3**. Since the second inflection in the titration curve is at an integral value ($a = 2$) and is concentration-independent the formation of a μ-hydroxo bridge between the two metal ions as suggested by the earlier workers[30a] can be ruled out. Thus complex **3** is completely different from that reported by Ezerskaya and Solovykh[30a] where a μ-hydroxo–μ-superoxo complex of Ru^{III}/Ru^{IV} was proposed.

Potentiometry of 1 in the Presence of 0.5 equiv of H_2O_2. The potentiometric titration curve of **1** in the presence of 0.5 equiv of H_2O_2 presented in Figure 1c shows a steep inflection at $a = 1$ and lies above the titration curve of the 1:1 H_2O_2 system (Figure 1d). In the buffer region $a = 0$–1 reactions 6 and 7 were assumed

$$2M^{III}LH + H_2O_2 \overset{K_6}{\rightleftharpoons} \underset{\mathbf{4}}{(HLM^{III})_2H_2O_2} \quad (6)$$

$$K_6 = [(HLM^{III})_2H_2O_2]/[M^{III}LH]^2[H_2O_2]$$

$$(HLM^{III})_2H_2O_2 \overset{K_7}{\rightleftharpoons} \underset{\mathbf{4a}}{(LM^{III})_2H_2O_2} + 2H^+ \quad (7)$$

$$K_7 = [(LM^{III})_2H_2O_2][H^+]^2/[(HLM^{III})_2H_2O_2]$$

to take place (L = EDTA). The constant log K_6 calculated by the spectrophotometric method is 9.0 ± 0.1. The value of the constant log K_7 is −6.60 ± 0.02.

The buffer region between $a = 1$ and $a = 3$ (Figure 1c) lies above those under nitrogen and oxygen (Figure 1a,b) and does not show any inflection beyond $a = 1$. The 1:0.5 curve (Figure 1c), however, lies below that of the 1:1 curve (Figure 1d). Reactions 8 and 9 were assumed to take place in the buffer region

$$(LM^{III})_2H_2O_2 + 2H_2O \overset{K_8}{\rightleftharpoons} \underset{\mathbf{4b}}{(LM^{III}OH)_2H_2O_2} + 2H^+ \quad (8)$$

$$K_8 = [(LM^{III}OH)_2H_2O_2][H^+]^2/[(LM^{III})_2H_2O_2]$$

$$(LM^{III}OH)_2H_2O_2 \overset{K_9}{\rightleftharpoons} \underset{\mathbf{4c}}{(LM^{III}(OH)_2)_2H_2O_2} + 2H^+ \quad (9)$$

$$K_9 = [(LM^{III}(OH)_2)_2H_2O_2][H^+]^2/[(LM^{III}OH)_2H_2O_2]$$

between $a = 1$ and $a = 3$ (L = EDTA). Constants corresponding to eq 8 and 9 calculated by on algebraic method are −19.0 ± 0.05 and −21.5 ± 0.05, respectively.

The structure of complex **4** as a μ-hydroperoxo–Ru(III) complex is supported by the sharp inflection at $a = 1$, corresponding to the formation of complex **4a**. Since there is no coordinated water molecule in **4**, there will not be any hydrolysis as in the case of the titration under nitrogen and oxygen. Complex **4a** undergoes hydrolysis beyond $a = 1$ to give the hydroxo–μ-hydroperoxo complex **4b** and further hydrolysis to the dihydroxo–μ-hydroperoxo species **4c**.

Potentiometry of 1 in the Presence of 1 equiv of H_2O_2. Potentiometric titration curve of **1** in the presence of 1 equiv of H_2O_2 is presented in Figure 1d. As in the case of the 1:0.5 H_2O_2 system (Figure 1c), the curve (Figure 1d) shows a steep inflection at $a = 1$, indicating the dissociation of a proton from the carboxyl group of complex **5** to give complex **5a**. Unlike the curve in the presence of 0.5 equiv of H_2O_2, the titration curve between $a = 0$ and $a = 1$ for the 1:1 H_2O_2 system exactly overlaps those under N_2 and O_2 (Figure 1a,b). This indicates a difference in the behavior of the systems in the presence of 0.5 and 1 equiv of H_2O_2, respectively.

The titration curve of **1** with 1 equiv of H_2O_2 (Figure 1d) overlaps with those of **1** under N_2 or O_2 (Figure 1a,b). This is because of the fact that there is no liberation of protons when **1** reacts with 1 mol of H_2O_2 (eq 10). In this case there is an

$$2(M^{III}LH) + 2H_2O_2 \overset{K_{10}}{\rightleftharpoons} \underset{\mathbf{5}}{(HLM^{IV})_2O_2^{2-}} + H_2O \quad (10)$$

$$K_{10} = [(HLM^{IV})_2O_2^{2-}]/[M^{III}LH]^2[H_2O_2]^2$$

apparent resemblence (overlap) between the three titration curves involving different species since the number of protons liberated is the same. In the case of interaction of **1** with H_2O_2, however, the formation of species **5** is deduced spectrophotometrically. Reactions 10 and 11 were assumed to take place in the buffer

$$(HLM^{IV})_2O_2^{2-} \overset{K_{11}}{\rightleftharpoons} \underset{\mathbf{5a}}{(LM^{IV})_2O_2^{2-}} + 2H^+ \quad (11)$$

$$K_{11} = [(LM^{IV})_2O_2^{2-}][H^+]^2/[(HLM^{IV})_2O_2^{2-}]$$

region $a = 0$–1 (L = EDTA; the charges on the complexes are omitted for the sake of clarity). The constant corresponding to eq 10 calculated by a spectrophotometric method is 11.0 ± 0.1. The constant K_{11} calculated by an algebraic method is −5.50 ± 0.05.

The buffer region between $a = 1$ and $a = 3$ (Figure 1d) lies above those under O_2 and N_2 and the 1:0.5 H_2O_2 system. As in the case of the 1:0.5 H_2O_2 system (Figure 1c) the titration curve in the 1:1 H_2O_2 system (Figure 1d) does not show any inflection beyond $a = 1$. In the buffer region $a = 1$–3, reaction 12 and 13

$$(LM^{IV})_2O_2^{2-} + 2H_2O \overset{K_{12}}{\rightleftharpoons} \underset{\mathbf{5b}}{(LM^{IV}OH)_2O_2^{2-}} + 2H^+ \quad (12)$$

$$K_{12} = [(LM^{IV}OH)_2O_2^{2-}][H^+]^2/[(LM^{IV})_2O_2^{2-}]$$

$$(LM^{IV}OH)_2O_2^{2-} + 2H_2O \overset{K_{13}}{\rightleftharpoons} \underset{\mathbf{5c}}{(LM^{IV}(OH)_2)_2O_2^{2-}} + 2H^+ \quad (13)$$

$$K_{13} = [(LM^{IV}(OH)_2)_2O_2^{2-}][H^+]^2/[LM^{IV}OH)_2O_2^{2-}]$$

were assumed to take place (L = EDTA). The constants cor-

Scheme I

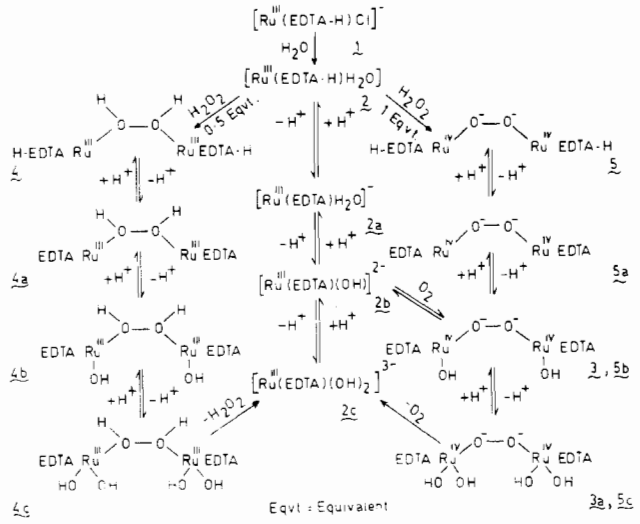

responding to eq 12 and 13 calculated by algebraic method are −19.4 ± 0.05 and −21.9 ± 0.05, respectively.

Complex **5a** undergoes hydrolysis to give complex **5b**, which undergoes further hydrolysis by the introduction of a second hydroxo group to give complex **5c**, identical with the reaction of complex **3a**. Complex **5c** undergoes an irreversible decomposition to give complex **2c** (Scheme I).

It was found that complex **4c** decomposes slowly as compared to **5c** or **3a** at higher pH ($a > 2.5$). This may be due to differences in the stability of the peroxo complexes of Ru(III) (complex **4c**) and Ru(IV) (complex **5c**) as reflected in their log K values.

The various equilibria found to exist in solution under nitrogen and oxygen and in the presence of H_2O_2 are shown in Scheme I.

Electrochemical Studies. In order to substantiate the assumptions based on potentiometric results, electrochemical studies of solution of **1** under nitrogen and oxygen and in the presence of 0.5 and 1 equiv of H_2O_2 respectively were investigated. Electrochemical studies were carried out with solutions corresponding to $a = 0.5$ (solution A), 1.5 (solution B), and 2.5 (solution C) of each of the titration curves of Figure 1, viz. curves a–d, respectively. The experimental solutions corresponding to Figure 1a are A1, B1, and C1, to Figure 1b are A2, B2, and C2, to Figure 1c are A3, B3, and C3, and to Figure 1d are A4, B4, and C4, respectively.

The differential-pulse polarograms (DPP) and cyclic voltammograms (CV) of solutions A1, B1, and C1 under nitrogen at the DME are presented in Figure 2. The reduction potentials ($E_{1/2}$), measured as the peak potentials in DPP at a modulation amplitude of 50 mV, are presented in Table I. The DPP of solution A1 containing species **2** and **2a** in equilibrium exhibits three reduction steps at −0.288, −0.842, and −1.012 V corresponding to one-electron reductions of Ru^{3+}/Ru^{2+}, Ru^{2+}/Ru^{+}, and the couple $H^+/^1/_2H_2$, respectively. Solutions B1 and C1 containing the hydroxo species **2b** and **2c** in equilibrium exhibit only one peak, corresponding to the Ru^{3+}/Ru^{2+} redox couple, with a shift in the potentials to more negative values up to −0.500 V. The shift of potentials to more negative values for solutions B1 and C1 under nitrogen is due to the formation of the monohydroxo and dihydroxo complexes **2b** and **2c**, respectively. This indicates an increase in the stability of the complexes with an increase in the number of coordinated hydroxo groups. Thus the stability follows the order MHL < ML < ML(OH). The potentials assigned to Ru^{3+}/Ru^{2+} in solutions A1, B1, and C1 are in good agreement with those reported by others.[33,37] The nonobservance of reduction steps for the Ru^{2+}/Ru^{+} and $H^+/^1/_2H_2$ couples in solutions B1 and C1 shows the absence of these redox reactions in basic solutions.

The CV of solutions A1, B1 and C1 (Table II) agree with those of the DPP results. The potential at −0.305 V ($0.5(E_{pa} + E_{pc})$) corresponds to the Ru^{3+}/Ru^{2+} redox couple. The reduction peaks at −0.842 and −1.012 V for Ru^{2+}/Ru^{+} and $H^+/^1/_2H_2$ couples,

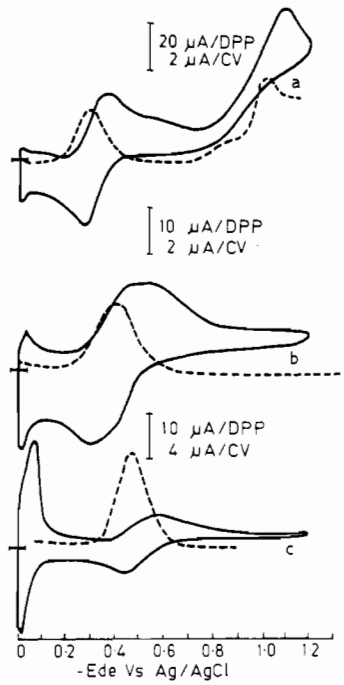

Figure 2. Differential-pulse and cyclic voltammograms of $K[Ru(EDTA\text{-}H)H_2O]\cdot 2H_2O$ (1×10^{-3} M) solution at 25 °C and $\mu = 0.1$ M KCl and at different a ([NaOH]/[ML]) values (a, 0.5; b, 1.5; c, 2.5) under nitrogen.

Table I. Polarographic Data for the Complex $K[Ru(EDTA\text{-}H)H_2O]\cdot 2H_2O$ at Different a ([NaOH]/[ML]) Values, with $t = 25$ °C and $\mu = 0.1$ M (KCl)[a]

		$-E_{1/2}$, V vs. Ag/AgCl		
no.	condition	soln A $a = 0.5$	soln B $a = 1.5$	soln C $a = 2.5$
1	N_2	0.288 0.842 1.012	0.405	0.475
2	O_2	0.300 0.860 1.055	0.220 0.375 0.520 0.660 0.920	(0.230) 0.440 (0.975)
3	H_2O_2 (1:0.5)[b]	0.370 0.630 0.990	0.260 0.435 0.598 0.765 1.060	0.510 0.640 0.850 1.111
4	H_2O_2 (1:1)[b]	0.805 0.980	0.358 0.475 0.680 0.960	0.645 0.875 1.120

[a] Values shown in parentheses refer to peak potentials for low peak currents. [b] Ratio of complex to H_2O.

respectively, in DPP are observed as a single overlapping step in CV at $-E_{pc} = 1.09$ V.

Figure 3 illustrates the electrochemical behavior (DPP and CV) of solutions A2, B2, and C2 under oxygen. The DPP of solution A2 exhibits three reduction steps at −0.300, −0.860, and −1.055 V as in the case of solution A1 under nitrogen (Figure 2a). Therefore, these peaks can be assigned to Ru^{3+}/Ru^{2+}, Ru^{2+}/Ru^{+}, and $H^+/^1/_2H_2$ couples, respectively. The CV of solution A2 is also similar to that of solution A1 under nitrogen. These results indicate that there is no interaction between complex **2** and oxygen in the acidic pH range (3.0–4.0), and the solution contains species **2** and **2a** in equilibrium.

The behavior of solution B2 under O_2 is however quite different from that of A2 in N_2, as shown by the DPP and CV evidence (Figure 3b). The DPP of solution B2 shows five peaks at −0.220,

Table II. Cyclic Voltammetric Data for the Complex K[Ru(EDTA-H)H_2O]·2H_2O at Different *a* ([NaOH]/[ML]) Values, with *t* = 25 °C and μ = 0.1 M (KCl)[a]

		soln A a = 0.5		soln B a = 1.5		soln C a = 2.5	
no.	condition	$-E_{pc}$, V	$-E_{pa}$, V	$-E_{pc}$, V	$-E_{pa}$, V	$-E_{pc}$, V	$-E_{pa}$, V
1	N_2	0.335	0.275	0.480	0.330	0.565	0.460
2	O_2	0.335	0.275	0.263	0.290	(0.265)	0.410
				0.420	(0.630)	0.535	
				0.615		(0.645)	
				0.675		(1.000)	
				0.995			
3	H_2O_2 (1:0.5)[b]	0.323	0.275	0.250	0.305	(0.400)	0.425
		0.500		0.385	(0.560)	0.670	
		0.588		0.610			
		0.902		0.700			
		1.080		1.050			
4	H_2O (1:1)[b]	0.304	0.233	0.212	0.268	(0.425)	0.500
		0.608		0.350	(0.605)	0.670	
		0.865		0.585		1.140	
		1.070		0.728			
				1.028			

[a] Values shown in parentheses refer to peak potentials for low peak currents. [b] Ratio of the complex to H_2O.

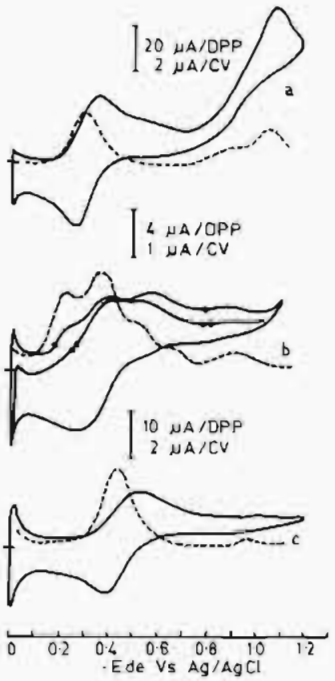

Figure 3. Differential-pulse and cyclic voltammograms of K[Ru(EDTA-H)H_2O]·2H_2O (1 × 10^{-3} M) solution at 25 °C and μ = 0.1 M KCl and at different *a* ([NaOH]/[ML]) values (a, 0.5; b, 1.5; c, 2.5) under oxygen.

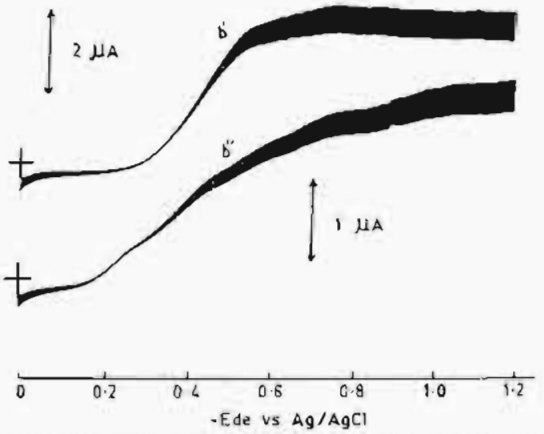

Figure 4. Direct-current polarograms of K[Ru(EDTA-H)H_2O]·2H_2O (1 × 10^{-3} M) solution at 25 °C and μ = 0.1 M KCl and at *a* ([NaOH]/[ML]) = 1.5 under (b′) nitrogen and (b″) oxygen.

Scheme II

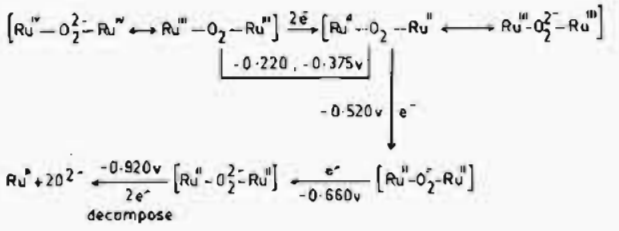

−0.375, −0.520, −0.660, and −0.920 V. The peaks at −0.22 and −0.375 V are in fact the two components of a single redox peak that can be assigned to the stepwise reduction of either the Ru^{4+}/Ru^{3+} or the Ru^{3+}/Ru^{2+} couple in complex **3** as shown in Scheme II. Such split peaks are characteristic of dimer formation[38] and are assigned to the stepwise reduction of either the Ru^{4+}/Ru^{3+} or the Ru^{3+}/Ru^{2+} couple as shown in Scheme II. In the formalism shown in Scheme II, it is not possible to distinguish between these redox states of the metal ion. If we start with the Ru(III)–O_2–Ru(III) species (Scheme II), which is equivalent to Ru^{IV}–O_2^{2-}–Ru^{IV}, a one-electron reduction per metal ion reduces the species to a formal Ru^{III}–O_2^{2-}–Ru^{III} or Ru^{II}–O_2–Ru^{II} species. The redox potential reported earlier[31] for Ru^{4+}/Ru^{3+}, −0.098 V, may be shifted to a more negative potential in the present case. These potentials are strongly dependent on pH and the number of protons released in a redox reaction.[39] A negative shift of −0.1 to −0.2 V is easily expected in these reactions since the dimer formation proceeds by the release of two protons. These data are supported by the polarogram of **2** (Figure 4b″).

Dimer **3** is a singly bridged μ-peroxo species without hydroxo bridging and does not contain any associated chlorides, as the starting species gets completely aquated in solution. It is thus completely different from the doubly bridged μ-peroxo–μ-hydroxo dimer reported earlier.[31] The doubly bridged dimer[31] may also contain some associated chloride ions. For this dimer we were able to observe[31] an anodic cathodic wave at −0.098 V. For dimer **3**, however, as explained above, no other anodic or cathodic wave

(38) Bhattacharya, S.; Chakravorty, A.; Cotton, F. A.; Mukherjee, R.; Schwotzer, W. *Inorg. Chem.* **1984**, *23*, 1709.

(39) Takeuchi, K.; Thompson, M. S.; Pipes, D. W.; Meyer, T. J. *Inorg. Chem.* **1984**, *23*, 1845.

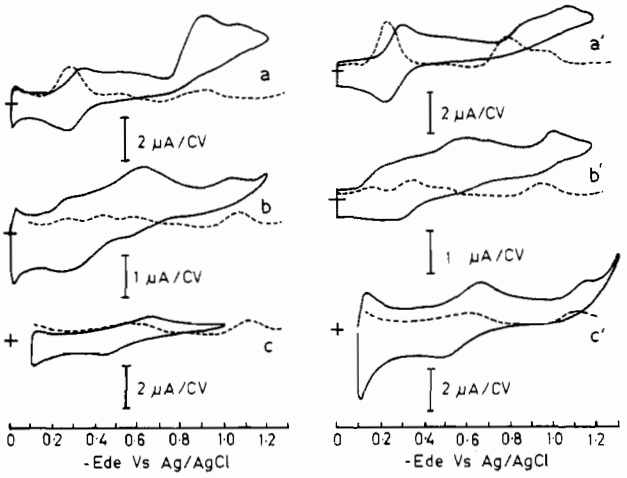

Figure 5. *Differential-pulse and cyclic voltammograms* of K[Ru(EDTA-H)H_2O]·$2H_2O$ (5×10^{-4} M) solution at 25 °C and $\mu = 0.1$ M KCl and at different a ([NaOH]/[ML]) values of 0.5 (a, a'), 1.5 (b, b') and 2.5 (c, c'). Curves a–c for voltammograms run in the presence of 0.5 in presence of half an equiv of hydrogen peroxide, and curves a'–c' are for those run in the presence of 1 equiv of hydrogen peroxide.

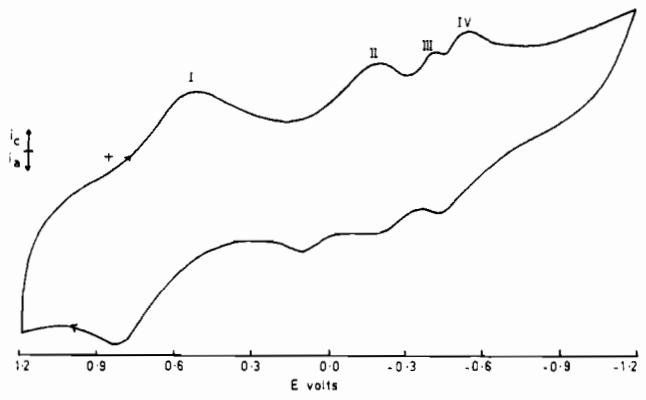

Figure 6. Cyclic voltammogram of the peroxo species [(H-EDTA)-$Ru^{IV}(O_2^{2-})Ru^{IV}$(EDTA-H)] in (1×10^{-3} M) solution in $\mu = 0.1$ M ($NaClO_4$) with a glassy-carbon working electrode and Ag/AgCl as reference electrode.

was observed in basic solution even when the polarogram was run on the positive side up to 1.0 V with a glassy-carbon electrode. The overall six-electron-redox process envisaged in Scheme II is also supported by coulometric studies conducted at −1.1 V on the cathodic side, which gives evidence for a three-electron reduction per metal center in going from dimer **3** to the decomposition product.

The peaks at −0.520 and −0.660 V of solution B2 under O_2 corresponding to species **3** are new and are not exhibited by solution A2 under O_2 or solution B1 under N_2, which contains species **2** and **2a** in equilibrium. These peaks correspond to the stepwise two-electron overall reduction of the coordinated O_2 in the species Ru^{II}–O_2–Ru^{II} to Ru^{II}–O_2^{2-}–Ru^{II} or the equivalent Ru^{III}–O_2^{2-}–Ru^{III} to Ru^{II}–O_2^{2-}–Ru^{II} (Scheme II).

The last peak at −0.920 V is somewhat broad and is assigned to a two-electron reduction of O_2^{2-} in the complex Ru^{II}–O_2^{2-}–Ru^{II} to O^{2-} and Ru^{II} (Scheme II). The peak due to the $H^+/^1/_2H_2$ couple, which is exhibited in solution A2, is absent in solution B2 because of the complete deprotonation of the complex **2a** beyond $a = 1$ (reaction 1). The reduction potentials of coordinated peroxide are in good agreement with those reported[40] for H_2O_2 (−0.8 V in 0.01 M HCl) and Et_2O_2 (−0.7 V in 0.1 M HCl).

The CV of solution B2 also exhibits five reduction peaks (Figure 3b and Table II). The first two peaks are due to the Ru^{3+}/Ru^{2+} couple as explained above, and the third and fourth peaks are due to reduction of coordinated oxygen as explained above. Whereas an anodic peak is exhibited for the Ru^{2+}/Ru^{3+} couple, the corresponding anodic peaks for other reductions could not be observed even at high scan rates, indicating the irreversible nature of these reactions.

The DPP of solution C2 under oxygen containing the species **3** and **3a** gives one reduction peak at −0.440 V (Figure 3c). This is due to the redox couple Ru^{3+}/Ru^{2+} of species **2c** formed by the irreversible decomposition of **3a**. The small peaks at −0.230 and −0.975 V may be assigned to the undecomposed dioxygen species **3a**.

The DPP of solution A3 in the presence of 0.5 equiv (Figure 5a) (species **4**) and 1 equiv of H_2O_2 (solution A4) (Figure 5a') (species **5**) show a behavior similar to those of solution A1 under nitrogen and solution A2 under oxygen (Table I). However, in the 1:1 H_2O_2 system (Figure 5a') the peaks lie at potentials positive of those of the 1:0.5 system (Figure 5a). This supports the formation of peroxo complexes of ruthenium **4**, **4a** and **5**, **5a** in the formal oxidation states of +3 and +4, respectively, in solutions A3 and A4, respectively. The potential of solution A4 shifts to more positive values because of the higher oxidation state (+4) of the metal ion in the μ-peroxo species **5**. This is in accord with a lower pH of the 1:1 curve (solution A4) as compared to the 1:0.5 curves (solution A3).

The CV of these solutions show two more unresolved peaks at −0.500, −0.588 V and −0.608, −0.865V for 1:0.5 and 1:1 systems, respectively. These peaks, which become more pronounced at higher pH, may be assigned to the peroxo group in complexes **4** and **5**, respectively.

The DPP and CV of solution B3 in 1:0.5 and solution B4 in 1:1 H_2O_2 systems (parts b and b' of Figure 5) containing species **4b** and **5b**, respectively, show a behavior similar to that of solution B2 (complex **3**) under oxygen. The DPP of solutions B3 and B4 exhibit five peaks (Table I) and the CV of the same systems also show five cathodic peaks (Table II) of which the first two are due to Ru^{3+}/Ru^{2+}, the third and fourth are due to coordinated H_2O_2/O_2^{2-}, and a fifth broad peak is due to the Ru^{2+}/Ru^{+} couple. The anodic peak in solutions B3 and B4 is similar to that of solution B2. Addition of a further 0.5 equiv of H_2O_2 converts solutions A3 and B3 to an equilibrium mixture of **5**/**5a** and **5a**/**5b**, respectively.

The electrochemical behavior of complex **5b** is thus the same as complex **3**, showing the identity of species prepared from two routes (O_2 and H_2O_2). When solution B4 was boiled and exposed to O_2 it absorbs O_2 as in the case of complex **3**. This was confirmed by the CV of solution B4 run on heating and on reabsorption of O_2 on cooling.

The DPP and CV of both the 1:0.5 and 1:1 H_2O_2 systems in solutions C3 and C4 (parts c – c' of Figure 5) containing species **4c** and **5c**, respectively, are similar to those of solution C2 (species **3a**) under oxygen, suggesting the presence of hydrolyzed Ru(III) species in 1:0.5 and 1:1 H_2O_2 systems, respectively. The electrochemical results of solutions B3 and C3 show that the species **4b** is more stable than **4c**, which decomposes in solution to **2c**.

Isolation and Characterization of the Solid Peroxo Complex [HLRu^{IV}(O_2^{2-})Ru^{IV}LH]. The complex [HLRu^{IV}(O_2^{2-})Ru^{IV}LH] (**5**, Scheme I) was precipitated as a green solid from the solution containing [Ru(EDTA-H)(H_2O)] in the presence of 1 equiv of H_2O_2 at pH 3.00 (solution A4) by the addition of alcohol. Alternatively the complex was precipitated from solution B2 at pH 7.5 by the addition of alcohol and redissolved in acid, the pH was adjusted to 3.00, and the complex was reprecipitated from the solution by alcohol. In both the cases the complex was obtained as a green solid, which analyzed as [(EDTA-H)Ru^{IV}(O_2^{2-})-Ru^{IV}(EDTA-H)] and decomposes without melting. The complex shows $\nu(O_2^{2-})$ at 870 cm^{-1} as a strong, sharp band characteristic of a coordinated peroxo group.

The CV of complex **5** in aqueous sodium perchlorate medium at pH 3.00 with a glassy-carbon electrode (Figure 6) gave peaks corresponding to the $E_{1/2}$ values at 0.67, −0.03, −0.16, and −0.46 V. The peaks observed at −0.675 and −0.995 V in the CV of complex **3** in basic medium (Table II) were not observed. The

(40) Odbrivskaya, A. A.; Neiman, M. B. *Acta. Physicochim. URSS* **1939**, *10*, 297; *Chem. Abstr.* **1939**, *33*, 6198.

Table III. Electronic Absorption Spectral Data for the Complex $K[Ru(EDTA\text{-}H)H_2O]\cdot 2H_2O$ at Different a ([NaOH]/[ML]) Values, with t = 25 °C and μ = 0.1 M (KCl)

		λ, nm (ε, M^{-1} cm^{-1})		
no.	condition	soln A a = 0.5	soln B a = 1.5	soln C a = 2.5
1	N_2	604 (53)	582 (45)	550 (23)
		573 (60)	522 (21)	299 (1499)
		280 (1862)	295 (1591)	222 (4169)
		224 (4182)	222 (4298)	
2	O_2	604 (53)	622 (105)	586 (45)
		573 (60)	390 (4581)	399 (990)
		279 (1941)	303 (1821)	296 (1571)
		224 (4285)	233 (4424)	237 (4492)
3	H_2O_2 (1:0.5)[a]	591 (164)	591 (162)	556 (140)
		557 (192)	556 (154)	399 (1414)
		392 (5124)	392 (5046)	299 (1919)
		303 (2116)	308 (2232)	215 (8360)
		220 (8282)	221 (8342)	
4	H_2O_2 (1:1)[a]	616 (180)	619 (168)	589 (126)
		556 (210)	611 (168)	399 (1486)
		391 (5850)	392 (5760)	299 (1903)
		303 (2288)	303 (2250)	215 (8360)
		222 (8460)	223 (8420)	

[a] Ratio of complex to H_2O_2.

peaks on the positive side disappear as previously stated when the CV was run with a glassy-carbon electrode at pH 9.0, indicating their shift to the negative side with pH. The peak at 0.67 V is assigned to the potential for the Ru^{4+}/Ru^{3+} couple. The peaks at −0.03 and −0.06 V are split peaks assigned to the reduction of the Ru^{3+}/Ru^{2+} couple. These peaks are observed in the CV of the alkaline solution (Table II, solution B2) at −0.263 and −0.420 V, respectively. The peak at −0.60 V, which is not well resolved, is assigned to the reduction of coordinated peroxo group in the said peroxo complex. The isolation and characterization of the peroxo complex **5** support all our experimental findings.

Spectrophotometry. Solution A1 under nitrogen shows two weak bands at 604 (ε 53) and 573 nm (ε 60) (all ε values in units of M^{-1} cm^{-1}) and two intense bands at 280 (ε 1862) and 224 nm (ε 4182). The band shifts to lower wavelengths (Table III) in solutions B1 and C1 are accompanied by a decrease in their intensity. The 573-nm band disappears in solution C1. The weak absorption bands at 604 and 573 nm may be assigned to the d–d transitions of Ru(III). The bands at 280 and 224 nm are the charge-transfer (CT) bands of EDTA and agree with those reported by Diamantis et al.[32] All the bands mentioned above are exhibited in solution A2 under oxygen and their intensities are almost the same. Thus molecular oxygen does not interact with complex **2** in solution A2.

Unlike solution B1, solution B2 under oxygen shows a band at 622 nm (ε 105) in place of bands at 582 (ε 45) and 522 nm (ε 21) (Table III) and new intense bands at 390 and (ε 4581) and 303 nm, respectively (Figure 7b). The charge-transfer band of EDTA was also observed at 233 nm. The bands at 303 (ε 1821) and 390 nm (ε 4581) are assigned[41] to the LMCT from the in-plane $1\pi^*_h$ and out-of-plane $1\pi^*_y$ components of the split $1\pi^*$ level of coordinated peroxide to a suitable acceptor d orbital on Ru(IV).[31,42] Similar LMCT bands were reported[39] for the monobridged μ-peroxo complexes of cobalt(III). The new band at 622 nm (ε 105) is assigned to Ru(IV) → O_2 MLCT.[42] The appearance of 303- and 390-nm bands for O_2^{2-} confirm the formation of the μ-peroxo Ru(IV) complex **3**. The bands are very close to those reported earlier.[30c] Similar charge-transfer bands at 380–390 nm were reported[39,43–46] for a number of (μ-peroxo)dicobalt(III) complexes. The d–d bands at 394 and 431 nm for Ru(IV) reported earlier[31] could not be observed due to the broad band at 390 nm, which extends over several nanometers and envelops the 394- and 431-nm bands. The band is thus a poorly resolved band, which may envelop along with it the LMCT from O_2 → M and the d–d transitions of Ru(IV).

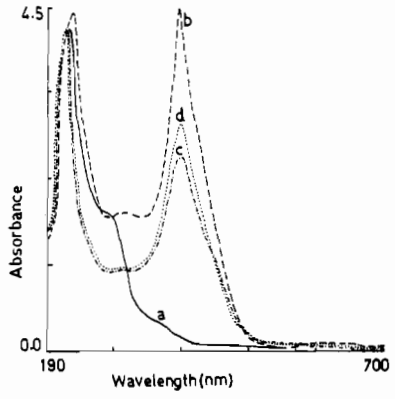

Figure 7. Absorption spectra of $K[Ru(EDTA\text{-}H)H_2O]\cdot 2H_2O$(ML) at 25 °C and μ = 0.1 M KCl: (a) [ML] = 1 × 10^{-3} M, under nitrogen; (b) [ML] = 1 × 10^{-3}, under oxygen; (c) [ML] = 5 × 10^{-4} M, [H_2O_2] = 2.5 × 10^{-4} M; (d) [ML] = 5 × 10^{-4} M, [H_2O_2] = 5 × 10^{-4} M.

Solution C2 under oxygen shows the same bands as in solution A2 under oxygen with the shifts shown in solution C1 under nitrogen. The peroxo bands at 303 and 390 nm and the Ru(IV) → O_2 MLCT band at 622 nm completely disappear, and a broad band centered at 399 nm (ε 990) appears along with the characteristic band for Ru(III) at 586 nm. The charge-transfer bands in the UV region at 225 and 280 nm are however affected to a small extent. This indicates that the oxygenated species in solution C2 decomposes irreversibly on increasing the pH and is converted to the dihydroxo–Ru(III) species **2c** as present in solution C1 under nitrogen.

The solution A3 in the presence of 0.5 equiv of H_2O_2 exhibits two weak d–d bands at 557 (ε 192) and 591 nm (ε 164), characteristic of Ru(III). The intensity of the 220-nm band is almost double that of the 224-nm band in solution A1 under nitrogen. In addition to these bands new bands appeared at 303 (ε 2116) and 392 nm (ε 5125), which may be assigned to $1\pi^*_h(H_2O_2)$ → Ru(III) and $1\pi^*_y(H_2O_2)$ → Ru(III), respectively (Figure 7c). This supports the interaction of H_2O_2 with complex **2** in solution A3 to form the Ru(III)–μ-hydroperoxo species **4**. The spectrum of solution B3 is the same as that of solution A3. In solution C3 the bands at 556 and 392 nm are reduced in intensity. The bands in the UV region at 215 and 399 nm are exhibited, but the 392-nm (peroxo) peak shifts to a broad peak at 399 nm with a decrease in intensity and resembles that of solution C2 under oxygen. This indicates a decomposition of species **4c** in solution to species **2c** and H_2O_2.

Solution A4 in the presence of 1 equiv of H_2O_2 exhibits peaks at 616 (ε 180), 391 (ε 5850), 303 (ε 2288), and 222 nm (ε 8460) while solution B4 shows peaks at 619 (ε 168), 392 (ε 5760), 303 (ε 2250), and 223 nm (ε 8420). The presence of bands at 616 and 619 nm in solutions A4 and B4, respectively, in place of the 591-nm band and the absence of Ru(III) bands at 557 nm show that the species formed in the 1:1 H_2O_2 system is the Ru(IV)–peroxo complex **5**. The peak around 620 nm characteristic of the Ru(IV) → O_2^{2-} MLCT band is also observed in the dioxygen complex **5**. As in the case of complex **3** the LMCT bands at 303 and 391 nm in complex **5** may be assigned to the $1\pi^*$ components of the LMCT of monobridged coordinated peroxo to Ru(IV). The characteristic green color of the peroxo complexes **3–5** is due to the absorption around 390 nm.

Effect of Heating of Solutions under Oxygen. When solution B2 boiled and cooled under nitrogen was subjected to electro-

(41) (a) McLendon, G.; Martell, A. E. *Coord. Chem. Rev.* **1976**, *19*, 1. (b) References 81, 92, 99, 155, and 156 in ref 35a.
(42) Lever, A. B. P.; Gray, H. B. *Acc. Chem. Res.* **1978**, *11*, 348.
(43) Miskowski, V. M.; Robins, J. L.; Treital, I. M.; Gray, H. B. *Inorg. Chem.* **1975**, *14*, 2318.
(44) Bosnich, B.; Poon, C. K.; Tobe, M. L. *Inorg. Chem.* **1966**, *5*, 1514.
(45) Bosnich, B.; Tobe, M. L. *Inorg. Chem.* **1965**, *4*, 1102.
(46) Huchital, D. H.; Martell, A. E. *Inorg. Chem.* **1974**, *13*, 2966.

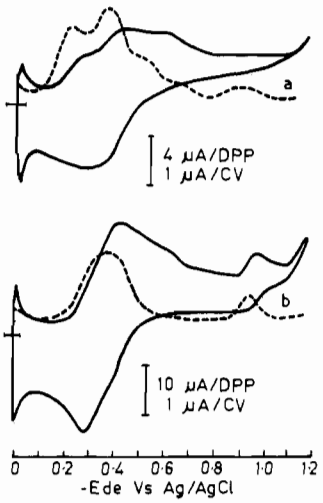

Figure 8. Differential-pulse and cyclic voltammograms of oxygenated $K[Ru(EDTA\text{-}H)H_2O]\cdot 2H_2O$ (1×10^{-3} M) solution of μ = 0.1 M KCl and at *a* ([NaOH]/[ML]) = 1.5: (a) at room temperature; (b) under hot conditions.

chemical studies, the DPP peaks at −0.375 and −0.920 V remained unaffected whereas those at −0.220, −0.520, and −0.660 V decreased in intensity (Figure 8). Similar observations were made for the CV also. The dc polarograms of the solution boiled and cooled under nitrogen were found to be similar to that of solution B1 under nitrogen (Figure 4). When these solutions were exposed to air and oxygen, the original DPP and CV (i.e. before boiling) were reproduced.

The absorption spectrum of solution B2 under oxygen also showed changes on boiling compatible with the results of DPP and CV. Figure 9 compares the spectra before and after boiling. Boiling of solution B2 causes a decrease in the intensity of the peaks at 622 and 390 nm with appearance of peak at 587 (ϵ 31) and 557 nm (ϵ 37) and a change in color of the complex from green to yellow. The peaks at 280 and 224 nm remain unaffected. The original spectrum of **3** was reproduced on exposing the solution to oxygen when the solution turns green.

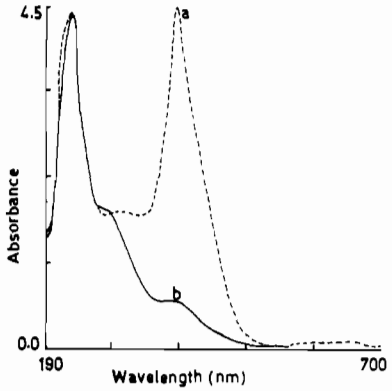

Figure 9. Absorption spectra of oxygenated $K[Ru(EDTA\text{-}H)H_2O]\cdot 2H_2O$ (1×10^{-3} M) solution at μ = 0.1 M KCl and at *a* ([NaOH]/[ML]) = 1.5: (a) at room temperature; (b) under hot conditions.

The electrochemical and spectrophotometric results thus support a reversible binding of dioxygen in complex **3**. Solution C2 does not exhibit this type of reversible behavior with oxygen.

Oxygen Absorption Studies. Solution A2 does not show any oxygen absorption. Thus oxygen does not react with complex **2** in acidic solution. In solution B2, however, absorption of oxygen was observed and the stoichiometry of dioxygen complex was found by the expression

$$N = N_r V / V_r$$

where N_r is the number of moles of oxygen bound per mole of reference complex $[(Ru^{III}EDTA)_2O_2(OH)]$ and V and V_r are volumes of oxygen absorbed by complex **2b** and reference, respectively, at constant temperature and pressure. The value of N was found to be 1. This supports the composition of complex **3** as a μ-peroxo species of Ru(IV). No absorption of oxygen was observed in solution C2.

Registry No. **1**, 76095-13-1; **2**, 15282-93-6; **2a**, 68122-22-5; **2b**, 66844-68-6; **2c**, 102682-51-9; **3**, 102682-52-0; **3a**, 102682-53-1; **4**, 102682-54-2; **4a**, 102682-55-3; **4b**, 102682-59-7; **4c**, 102682-58-6; **5**, 102682-56-4; **5a**, 102682-57-5.

Contribution from the Departments of Chemistry, Portland State University, Portland, Oregon 97207, and University of Idaho, Moscow, Idaho 83843

Oxidative-Addition/Addition Reactions of *F-tert*-Butyl Hypochlorite with Perfluoromono- or Perfluorodiiodoalkanes, Pentafluoroiodobenzene, and Hexafluorobenzene

Jo Ann M. Canich,[1a] Megan E. Lerchen,[1a] Gary L. Gard,*[1a] and Jean'ne M. Shreeve*[1b]

Received March 21, 1986

At 0 °C, $(CF_3)_3COCl$ undergoes oxidative addition reactions with CF_3I, ICF_2CF_2I, $SF_5CF_2CF_2I$, and C_6F_5I to form $CF_3I[OC(CF_3)_3]_2$, $[(CF_3)_3CO]_2ICF_2CF_2I[OC(CF_3)_3]_2$, $SF_5CF_2CF_2I[OC(CF_3)_3]_2$, and $C_6F_5I[OC(CF_3)_3]_2$, respectively. In a further reaction of the latter with $(CF_3)_3COCl$, addition to the ring occurs to form $[(CF_3)_3CO]_2IC_6F_5[(CF_3)_3CO]_2Cl_2$. With C_6F_6, $(CF_3)_3COCl$ gives $C_6F_6[OC(CF_3)_3]_2Cl_2$. The new compounds are stable viscous liquids or low-melting solids.

Introduction

The reactions of hypochlorites continue to attract the attention of chemists who are interested in new materials. Trifluoromethyl hypochlorite and *F-tert*-butyl hypochlorite have been studied most thoroughly, and while they both undergo oxidative addition and/or oxidative displacement reactions in general, $(CF_3)_3COCl$ has the advantage over CF_3OCl as a synthetic reagent because it does not also act indirectly, via its decomposition, as a fluorinating agent. It is interesting to note that with the exception of the reaction of $(CF_3)_3COCl$ with SO_2 to form $(CF_3)_3COSO_2Cl$, there are no examples of its oxidative-addition reactions in which the highest possible oxidation state of the central element is formed, e.g.: S(0) → S(IV), S(II) → S(IV); I(0) → I(III); Te(0) → Te(IV); Pb(O) → Pb(II); Bi(0) → Bi(III).[2-6] In this paper, we

(1) (a) Portland State University. (b) University of Idaho.

(2) Young, D. E.; Anderson, L. R.; Fox, W. B. *Inorg. Chem.* **1971**, *10*, 2810.

0020-1669/86/1325-3030$01.50/0